Structure and cation dynamics in the system $AgI:Ag_2MoO_4$: A ^{109}Ag NMR study

Piercarlo Mustarelli,* Corrado Tomasi, Eliana Quartarone, and Aldo Magistris
C.S.T.E.-C.N.R. and Department of Physical Chemistry, University of Pavia, Via Taramelli 16, 27100 Pavia, Italy

Maria Cutroni and Andrea Mandanici
Department of Physics, University of Messina and Unità INFM, ctr. Sperone, 98100 Messina, Italy
(Received 6 February 1998)

The system $(AgI)_{1-x}(Ag_2MoO_4)_x$ is studied with ^{109}Ag solid-state NMR and differential scanning calorimetry. Glasses are formed for $0.2<x<0.4$. Outside the glass formation region a glassy phase of molar composition 0.66 AgI-0.33 Ag_2MoO_4 is always found, which is accompanied by β-AgI or Ag_2MoO_4 crystals. Upon thermal treatments above 120 °C, a 0.66 AgI-0.33 Ag_2MoO_4 (2:1) phase crystallizes over the entire composition range. The chemical shift anisotropy tensor of this phase has been assigned. The anisotropy is ~70 ppm, that is an order of magnitude lower than the isotropic chemical shift range observed in silver borate glasses. The addition of AgI to Ag_2MoO_4 causes the formation of oxy-iodide sites. The existence of AgI clusters can be ruled out. Spin-lattice relaxation inside the glass-formation region seems to be controlled by Ag-I scalar coupling of the first kind, rather than by chemical shift anisotropy. The existence of two maxima in the spin-lattice relaxation rate curve points towards Ag^+ populations with different mobility.
[S0163-1829(98)05537-4]

I. INTRODUCTION

Silver molybdate glasses, $AgI:Ag_2O:MoO_3$, are known to be fast ionic conductors.[1,2] At present, researchers' interest is stimulated not only by the extremely high conductivity which reaches $\sim 10^{-2}\Omega^{-1}$ cm^{-1} at room temperature, but also, from a basic point of view, by the growing evidence of anomalies in the structure as well as in their intensive properties when compared with silver borate and silver phosphate glasses.

Minami and Tanaka[3] showed that glasses with a mole ratio $Ag_2O/MoO_3=1$ contained no condensed macroanions, but only discrete Ag^+, I^-, and MoO_4^{2-}. In their model only a part of the silver ions are believed to participate in the conduction.

Almond, Duncan, and West[4] reported that the conductivity of a glass 0.75 AgI-0.25 Ag_2MoO_4 (3:1) is due to the anomalous high prefactor caused by the magnitude of the ion hopping rate. The effective attempt frequency of the hopping process appeared to be as high as 10^{15} s^{-1}, chiefly because of the effects of activation entropy. St. Adams, Hariharan, and Maier[5] recently pointed out that the conductivity enhancement during crystallization of the same glass can hardly be attributed to interfacial effects, as it was found in phosphate and vanadate glasses.

Diffractometric and spectroscopic evidences of anomalies in 3:1 glass have been also reported. Swenson *et al.*[6] showed by neutron-diffraction coupled with reverse Monte Carlo method that the origin of the first sharp diffraction peak arising in the 3:1 glass is somewhat different from that of borate and phosphate glasses, and cannot be simply explained in term of AgI clustering. Finally, Kamitsos *et al.*[7] showed by infrared spectroscopy that the Ag^+ motion frequency in molybdate glasses remains relatively unaffected by the AgI content, in contrast to what happens in borates and phosphates.

In summary, some relevant questions appear to be still open about silver molybdate glasses and, among the others, those concerning: (i) the existence of one or more distinct Ag^+ populations with different mobility, (ii) the growth of AgI clustering with associated diffusion pathways, (iii) the glass forming ability of the molybdate, and (iv) the existence of local composition fluctuations.

^{109}Ag solid-state NMR is a powerful technique to study glassy electrolytes for its capability to discriminate among chemically different Ag^+ ions because of the large chemical shift ($\delta\sim 1000$ ppm) of silver, and to obtain unique information on ion dynamics through line-narrowing and spin-lattice relaxation. However, these applications are strongly limited by the poor signal-to-noise ratio of the ^{109}Ag signal in the solid state, and by the interpretative difficulties of NMR data, chiefly because little is known about the chemical shift tensor in silver compounds. To date, in fact, only a few ^{109}Ag NMR papers appeared about silver borates,[8–11] whereas nothing has yet appeared about molybdates, to our knowledge.

In this paper we present a detailed ^{109}Ag NMR analysis on the pseudobinary system $(AgI)_{1-x}(Ag_2MoO_4)_x$. We study both structure and cation dynamics inside, as well as outside, the glass-formation region, which covers the range $0.2<x<0.4$ as can be appreciated in Fig. 1 (see caption for more details). The spin interactions that determine both linewidth and spin-lattice relaxation mechanism are discussed. We correlate our NMR data with both out-of-phase and equilibrium phase diagrams we recently discussed,[12] which are reported in Fig. 1. In particular, the possible formation of a glassy phase of composition 0.66 AgI-0.33 Ag_2MoO_4 (2:1) over the entire composition range will be discussed.

II. EXPERIMENTAL DETAILS

Glassy or partially glassy samples of the $(AgI)_{1-x}(Ag_2MoO_4)_x$ system (with $x=0.1$; 0.2; 0.25; 0.33;

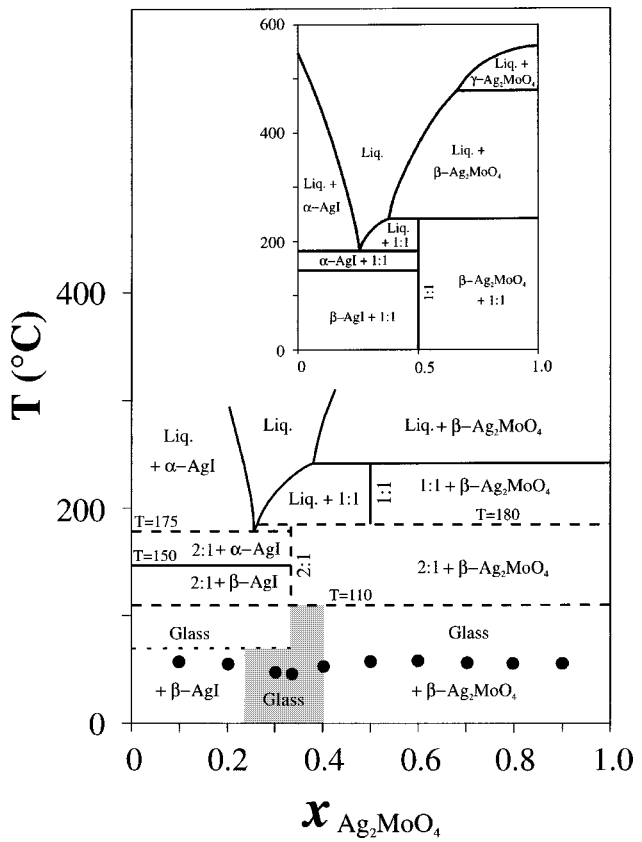

FIG. 1. Phase diagram of AgI:Ag_2MoO_4 system. The inset represents the equilibrium part. The shaded area indicates the glass-formation region. The dashed lines give metastable phases boundaries. The dotted line at 70 °C represents further nucleation of β-AgI in a composition range where crystalline β-AgI is already present in the as-quenched samples. Filled circles indicate the T_g's. In the case of $x=0.40$, just the average value of the two observed T_g's is displayed.

0.4; 0.5; 0.6; 0.7; 0.8; 0.9) were prepared by the melting-quenching technique. Appropriate mixtures of AgI (Aldrich 99%) and Ag_2MoO_4 [prepared by precipitation from aqueous solution of $AgNO_3$ and Na_2MoO_4 (Ref. 13)], were melted at 600 °C for 2 h in quartz tubes and then quenched down to room temperature (rt) in stainless-steel molds.

^{109}Ag solid-state NMR spectra were acquired on a AMX400WB spectrometer (Bruker, Germany), at a Larmor frequency of 18.61 MHz, with a wideline probe (Bruker, Germany). The spectra were referenced to a 10 wt. % aqueous solution of $AgNO_3$. A 90° pulse of 10 μs, a repetition time varying from 100 to 500 s, and a bandwidth of 200 kHz were chosen. Up to ~160 accumulations were needed to obtain acceptable S/N ratios. The spectra were obtained both by single-pulse and Hahn-echo sequences. Care was taken to avoid signal saturation and to minimize baseline distortions. T_1 values were obtained from a conventional saturation-recovery sequence.

Differential scanning calorimetry measurements (DSC) were run with a 2910 DSC controlled by a TA 2000 system (TA Instruments). All experiments were performed on powdered samples, in crimped silver pans, at a rate of 10 °C/min under dry N_2 purge. The temperatures of the thermal phenomena are affected by an uncertainty of ±2 °C.

Powder x-ray-diffraction patterns were taken on a Philips PW 1710 powder diffractometer, equipped with a Philips PW 1050 vertical goniometer and a graphite crystal monochromator (Cu $K\alpha$ radiation).

III. THEORETICAL BACKGROUND

The NMR chemical shift is due to the screening of the applied magnetic field at a given nucleus by the surrounding electrons. The Hamiltonian of interaction to be added to the Zeeman term has the form[14]

$$\hbar H_{\mathrm{CS}} = \gamma_I \hbar \mathbf{I} \sigma \mathbf{B}_0, \tag{1}$$

where $\mathbf{I}$ is the nuclear spin, γ_I is the gyromagnetic ratio, $\mathbf{B}_0$ is the applied external magnetic field, σ is the screening second-rank tensor, and the other symbols have the usual meaning. In the first-order perturbation theory, the chemical shift contribution to the resonance frequency is given by the secular part of the Hamiltonian

$$\mathbf{H}_{\mathrm{CS}}^{\mathrm{sec}} = \gamma_I B_0 I_z \sigma_{zz} \tag{2}$$

with

$$\sigma_{zz} = \sigma^* + \frac{1}{2}\,\sigma_{\mathrm{CS}}(3\cos^2\,\theta - 1 + \eta_{\mathrm{CS}}\sin^2\,\theta\,\cos 2\varphi), \tag{3}$$

where θ and φ are the Euler angles, and σ^*, δ_{CS}, and η_{CS} are the isotropic shielding, the anisotropy, and the asymmetry parameter, respectively. They are expressed in terms of the eigenvalues of the diagonalized screening tensor

$$\sigma^* = \frac{1}{3}\,\mathrm{Tr}\sigma = -\frac{1}{3}\,(\sigma_{11}+\sigma_{22}+\sigma_{33}), \tag{4}$$

$$\delta_{\mathrm{CS}} = \sigma_{33} - \sigma^*, \tag{5}$$

$$\eta_{\mathrm{CS}} = \frac{\sigma_{22}-\sigma_{11}}{\sigma_{33}-\sigma^*} \tag{6}$$

under the convention $\sigma_{33} > \sigma_{22} > \sigma_{11}$, for which $0 \leqslant \eta_{\mathrm{CS}} \leqslant 3$. The resonance frequency of a NMR experiment is given by

$$\nu = \nu_L(1-\sigma_{zz}), \tag{7}$$

where ν_L is the Larmor frequency of the unscreened nucleus. The σ scale is related to the δ scale, which is of common use in high-resolution NMR, by the relation $\delta \cong -\sigma$.

In polycrystalline as well as in amorphous materials all orientations of σ arise with equal probability, and we have a random distribution of the Euler angles in Eq. (3). This leads to characteristic wide-line spectra called chemical shift anisotropy (CSA) powder patterns. The general case of $\eta_{\mathrm{CS}} \neq 0$ cannot be expressed by closed algebraic relations: the involved calculations were reported by Bloembergen and Rowland.[15]

The spin-lattice relaxation, $1/T_1$, determined by the modulation of the anisotropic screening tensor for the ionic motion is given by[16]

$$\left(\frac{1}{T_1}\right)_{\mathrm{CSA}} = \frac{\mu_0}{60\pi}\,\gamma_I^2 B_0^2 \Delta\sigma^2 \left(\frac{2\tau_c}{1+\omega_I^2\tau_c^2}\right), \tag{8}$$

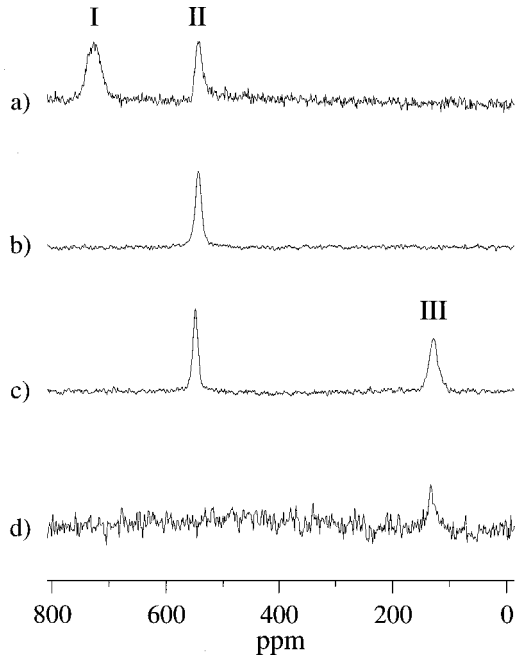

FIG. 2. ^{109}Ag NMR spectra at room temperature of the samples $x=0.1$ (a), $x=0.33$ (b), $x=0.7$ (c), and $x=1$ (d). The labels I, II, and III indicate β-AgI, a glassy phase and crystalline Ag_2MoO_4, respectively (see text).

where ω_1 is the Larmor frequency of the spin **I** and τ_c is a characteristic jump time for the ions. In the motional narrowing limit we have

$$\left(\frac{1}{T_1}\right)_{\mathrm{CSA}}=\frac{\mu_0}{30\pi}\,\gamma_I^2 B_0^2 \Delta\sigma^2 \tau_c \tag{9}$$

and the relationship $(T_1)_{\mathrm{CSA}}/(T_2)_{\mathrm{CSA}}=7/6$ holds.[16]

If the spin-lattice relaxation is determined by scalar coupling of the spin **I** with another spin **S**, we have

$$\left(\frac{1}{T_1}\right)_{\mathrm{SC}}=\frac{8\pi^2 J^2 S(S+1)}{3}\left[\frac{\tau_{\mathrm{SC}}}{1+(\omega_I-\omega_S)^2\tau_{\mathrm{SC}}^2}\right], \tag{10}$$

where J is the scalar coupling constant between **I** and **S**, S is the quantum spin number, $\omega_{I,S}$ are the Larmor frequencies of the two spins at the given magnetic field, and τ_{SC} is a characteristic time which depends on the kind of modulation. If the coupling is modulated by diffusion (relaxation of first kind) τ_{SC} has the meaning of a jump time. If the coupling is modulated by fast relaxation of spin **S** ($S>1/2$, relaxation of the second kind) τ_{SC} is given by the T_1 of the relaxing spin S.

IV. STRUCTURAL INFORMATION

The isotropic chemical shift

Figure 2 shows some representative NMR spectra recorded over the entire composition range, and namely those of the samples $x=0.1$ (a), $x=0.33$, (b), $x=0.7$ (c), and $x=1$ (d). The sample $x=0.1$ displays two peaks at 728 and 544 ppm, which are labeled as I and II, respectively. The former is attributed to AgI for its chemical shift,[8] whereas the latter is likely that of a residual phase of composition $0.66\mathrm{AgI}\cdot 0.33\mathrm{Ag_2MoO_4}$ (2:1). This attribution has been made by comparing the areas of the NMR peaks with the theoretical values (reported in Table I) obtained under the assumption that the maximum allowable fraction of 2:1 phase is formed at each composition. We assume that this last phase is a glass, since the x-ray-diffraction pattern of sample $x=0.1$ shows only the reflections of β-AgI (compare Fig. 1), whereas its DSC thermogram (not reported here) highlights a clear glass transition.[12]

The NMR spectrum of the sample $x=0.33$ (b) shows a single peak at 544 ppm (labeled as peak II), whereas $x=0.7$ (c) is characterized by two peaks at 548 and 127 ppm, which are labeled as II and III, respectively. The peak at

TABLE I. The peak numbering refers to the labels of Fig. 2. The chemical shift (CS) and the full width at half height (FWHH) have an uncertainty of ±3 ppm. The areas have an uncertainty of ±5%. The area values reported in the section ''2:1 formation (theoretical)'' have been obtained by supposing the maximum formation of the 2:1 glassy phase for each nominal composition outside the glass-formation region.

Samples	Peak I			Peak II			Peak III			Center-of-mass	2:1 formation (theoretical)		
x (molar fraction)	CS (ppm)	FWHH (ppm)	Area (%)	CS (ppm)	FWHH (ppm)	Area (%)	CS (ppm)	FWHH (ppm)	Area (%)	CS (ppm)	Area Peak I (%)	Area Peak II (%)	Area Peak III (%)
0.1	728	30	65	544	15	35				663	64	36	
0.2	733	30	38	551	18	62				620	33	66	
0.25				564	8	100				564			
0.33				543	10	100				543			
0.4				528[a]	9	90	127	19	10	488		86	14
0.5				548	10	74	127	18	26	439		67	33
0.6				548	12	62	127	16	38	388		50	50
0.7				549	10	39	127	16	61	292		35	65
0.8				548	10	13	127	17	87	181		22	78
0.9				548		2	127	17	98	135		11	89
1.0							130	17	100	130			

[a]The value indicated by the center-of-mass of the two peaks reported in Fig. 5.

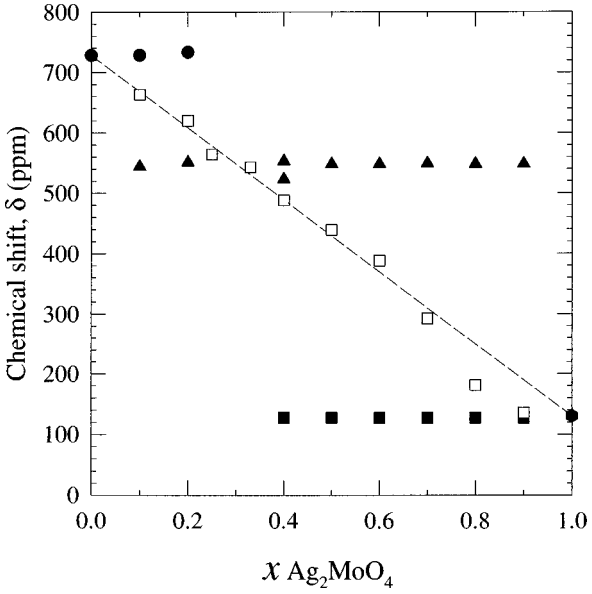

FIG. 3. ^{109}Ag NMR chemical shifts vs the composition parameter x of the peaks observed in all the samples studied. Filled circles represent crystalline AgI. Filled triangles represent a glassy phase. Filled squares represent crystalline Ag_2MoO_4. Open squares represent the positions of the spectra centers-of-mass. The dashed line is the position of the center-of mass if each sample is an ideal mixing of the constituents.

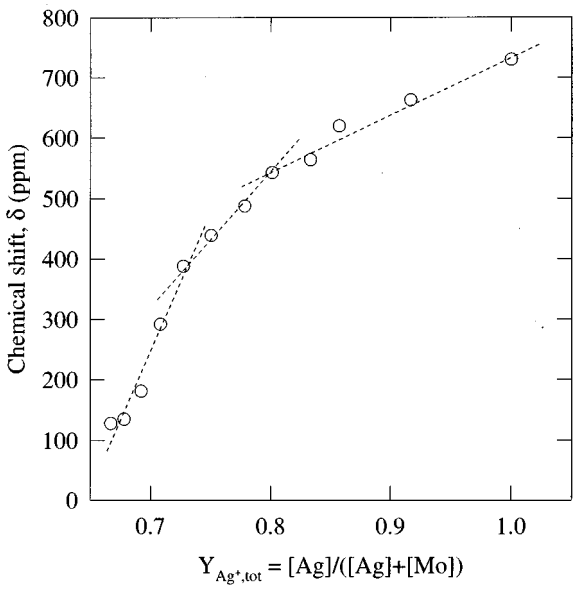

FIG. 4. ^{109}Ag NMR chemical shift of the centers-of-mass against the total silver cationic molar fraction, $Y_{\mathrm{Ag,tot}}$. Dashed lines are linear best fits.

higher field (III) is attributed to Ag_2MoO_4; in fact, it is nearly at the same position of the single peak observed for $x=1$ in Fig. 2(d). The peak at 548 ppm is again due to a glassy phase of composition 2:1, as it is demonstrated by the areas ratio reported in Table I, by DSC measurements,[12] and by x-ray-diffraction data (not reported) which show only the reflections of crystalline Ag_2MoO_4. Peaks at the same position, and with nearly the same width, of those of Fig. 2(c) are observed in all the samples in the range $0.5 \leqslant x \leqslant 0.8$ (see Table I). We stress here that the mechanisms controlling the width of the two peaks are different: in fact, the peak at 548 ppm is narrowed because of the high ion dynamics of the glassy phase, whereas the width of the peak at 127 ppm is determined by the distribution of chemical shift in the silver molybdate crystal. This is confirmed by the longitudinal relaxation times, T_1, which at rt are $\sim$1 s for the peak at 548 ppm, and $\sim$300 s for the peak at 127 ppm.

Figure 3 shows the chemical shifts of all the as-quenched samples vs x. Inside the glass-formation region a single peak is observed. To the left of the glass-formation region, $x \leqslant 0.2$, the samples are phase-separated into AgI (filled circles) and 2:1 glass (filled triangles). To the right of the glass-formation region, $x \geqslant 0.4$, the samples are again phase-separated into 2:1 glass and Ag_2MoO_4 (filled squares). Two glassy phases are observed in the sample $x=0.4$ (see following). Open squares represent the center-of-mass of the spectra; inside the glass-formation region they coincide with the observed single peak. The dashed line which connects the positions of AgI (728 ppm) and Ag_2MoO_4 (130 ppm) represents the chemical shift each sample would show if it was a coarse mixture of the constituting compounds, e.g., AgI and Ag_2MoO_4. We stress that the reason why the chemical shift of the 2:1 phase is located nearly at one third of the way between those of AgI and Ag_2MoO_4 is that each Ag^+ experiences, in its coordination sphere, a statistical iodine/oxygen ratio that changes quasilinearly in the region of interest. Apparently, our data fit well the dashed line for $x \leqslant 0.6$, while a dispersion is found for higher values of the composition parameter x.

In order to investigate the chemical shift nonlinearity of the center-of-mass, we can plot the data against the total silver cationic molar fraction, $Y^+_{\mathrm{Ag,tot}}$=[Ag]/([Ag]+[Mo]), see Fig. 4. Two neat slope changes become evident at $y \cong 0.73$ and at $y \cong 0.80$, which correspond to $x \cong 0.6$ and $x \cong 0.33$, respectively. Villa *et al.* found a knee at $x=0.6$ in silver borate glasses.[8] They argued that the knee corresponds to the maximum AgI fraction for which it is possible to have each silver coordinated to one iodine, and each iodine surrounded by four silver ions. In their picture, further addition of AgI resulted in formation of structures with more than one iodine coordinated to Ag^+. Nonlinearities of ^{109}Ag chemical shifts values have been recently reported by Sanz *et al.* in silver tellurite glasses.[17]

To explain our results we recall that our center-of-mass is the average of Ag^+ belonging to crystalline phases (Ag_2MoO_4 or β-AgI), and of a fraction belonging to the 2:1 glassy phase. As a consequence, the NMR signal may reflect the Ag^+ local dynamics in addition to well-defined molecular or crystallographic structures. This is consistent with the strongly depolymerized model proposed by Minami for silver molybdate glasses.[18,19] When small quantities ($<$10 mol %) of AgI are added to Ag_2MoO_4, the averaged local field seen by silver molybdate is just marginally modified. As a result, our center-of-mass value strongly overestimates the crystal fraction, and this accounts for the anomaly well-evident in Fig. 3 for $x=0.9$, and still appreciable in Fig. 4. For $x \leqslant 0.8$ the average time for which a fraction of the Ag ions ''see'' I^- becomes longer than the NMR time scale and the signal of the oxyiodide structures (-O-Ag-I-) of the 2:1 glassy phase arises.

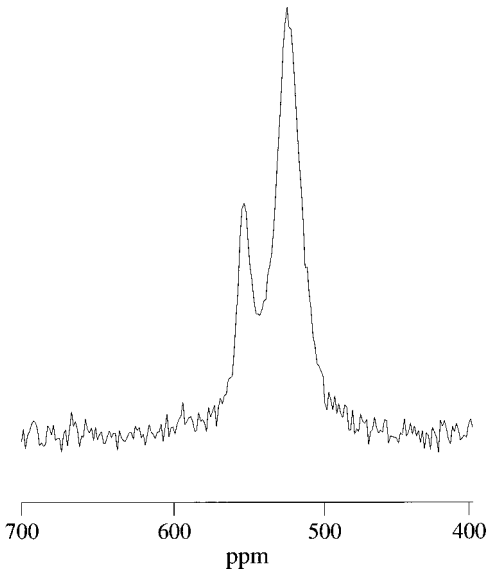

FIG. 5. ^{109}Ag NMR spectrum at room temperature of the sample $x=0.4$ as-prepared.

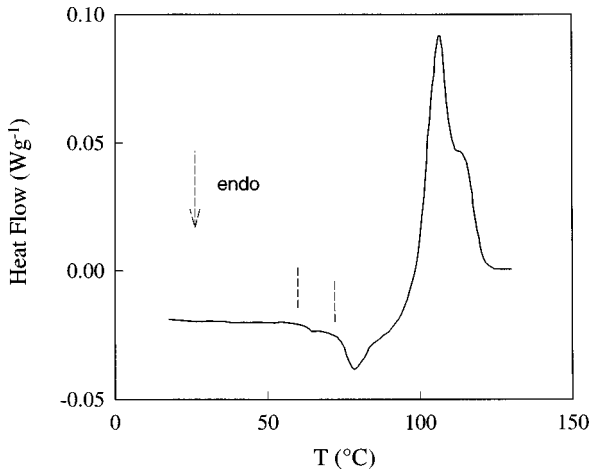

FIG. 6. DSC thermogram of the sample $x=0.4$ as-prepared. The T_g's are indicated by dashed lines. The dashed arrow indicates the endothermic direction.

For $0.8 \geqslant x \geqslant 0.6$, the fraction of I^- that are dynamically ''seen'' by each Ag^+ increases more and more and reaches the ratio 1:4. For $x=0.6$ each Ag^+ ''sees'' one iodine in its coordination sphere. Villa *et al.*[8] demonstrated that the substitution of one oxygen with one iodine determines an increase of ~300 ppm in the Ag^+ chemical shift, which is nearly the same variation we measure from $x=1$ to $x=0.6$ (see Fig. 3). For $x<0.6$ a second iodine enters the Ag^+ coordination sphere, and the average chemical shift changes with a lower slope. For $x=0.33$ the ratio I:Ag is 0.5, that means that each Ag^+ experiences, in average, two I^- in its coordination sphere. The second O/I substitution roughly accounts for a chemical shift change of ~150 ppm. Finally, for $0.33 > x \geqslant 0$ the fraction of iodine seen by each Ag^+ ranges from 50 to 100%. However, we have not enough experimental points to appreciate the difference between the presence of three or four I^- in the Ag^+ coordination sphere. Furthermore we recognize that our discussion is only qualitative, because of the low number of experimental points and their scattering, and also since they are often the average over several phases.

Another question arises about the structure of the samples inside the glass-formation region. In fact, a single NMR peak may be observed for one of the following reasons: (i) the glassy phase is really homogeneous, in the sense that all the Ag^+ ''see'' the same chemical environment (no composition fluctuations), or (ii) the cation dynamics is fast enough to average spectral lines with different chemical shift. As a matter of fact, subliquid immiscibility with spatial fluctuations of the order of 10 nm was supposed to exist in $AgI:Ag_2O:B_2O_3$ glasses.[8] Some information may be obtained by a careful study of the sample $x=0.4$, which is at the boundaries of the glass-formation region. The spectrum of $x=0.4$, reported in Fig. 5, displays two partially overlapped peaks centered at 553 and 523 ppm, respectively, and the peak of Ag_2MoO_4 at 127 ppm (not shown in the figure). This last peak accounts for ~10% of the NMR total intensity. Since x rays show only some weak reflections of Ag_2MoO_4, we believe that the two high-frequency peaks correspond to two glassy phases. If we suppose that the actual composition of the glassy part is near to 0.64 AgI-0.36 Ag_2MoO_4, from the NMR areas ratio we obtain for the two phases the values $x \cong 0.31$ and $x \cong 0.38$, which are also in agreement with the chemical shift dependence displayed in Fig. 3.

The existence of two glassy phases, one of which very near to the 2:1 ratio, is further supported by the DSC thermogram of Fig. 6 that shows two T_g's at 60 and 74 °C. The correlation we find between the glass transition temperature and the supposed glass stoichiometry is in agreement with the thermal data reported by Kawamura and Shimoij[20] and Minami, Nambu, and Tanaka[2] for compositions similar to those we are here hypothesizing. The two partially overlapped exothermic peaks in the temperature range 90–120 °C represent the cold crystallizations of the two glassy phases. We may conclude that the Ag^+ local coordination of the 2:1 glassy structure seems to be privileged over the entire composition range, as also supported by the x-ray-absorption near-edge structure data, on $x=0.25$ and $x=0.33$ reported in Ref. 21.

The anisotropic part of the chemical shift

It is well accepted that the spin interaction dominating the ^{109}Ag NMR line shape in silver oxysalt glasses is the chemical shift.[8,10] While at rt the NMR line is generally narrowed by ionic motion, it is not clear if the broad features (up to 10 kHz, i.e., 620 ppm) observed at low temperatures in borate glasses[10] are simply a result of a wide distribution of isotropic chemical shifts or does the anisotropic part contribute as well. As a matter of fact, we are here reporting an isotropic chemical shift range of the order of 600 ppm, whereas Looser and Brinkmann found shifts in the range 700–800 ppm for $RbAg_4I_5$ and KAg_4I_5,[22] and Burges *et al.* obtained shift values around 0 ppm for silver oxyanions in aqueous solution.[23]

Figure 7 reports the NMR spectra at room temperature of the samples $x=0.33$ (a) and $x=0.25$ (b), heated in a oven at 140 °C for 15 h. The spectrum (a) consists of a pattern of chemical shift anisotropy (CSA), which we assign to the 2:1 crystallized phase, according with the x-ray-diffraction data

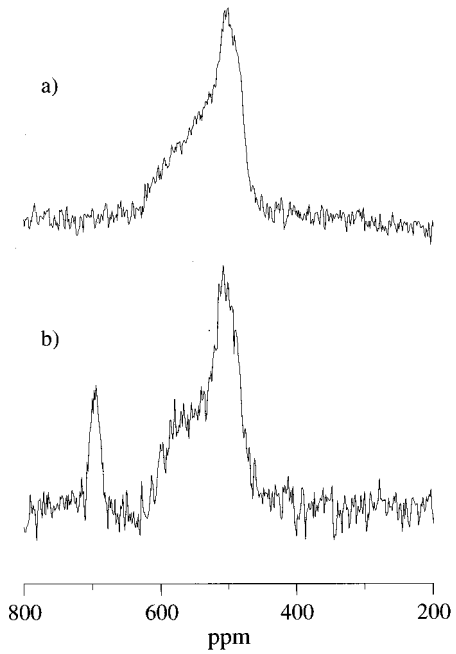

FIG. 7. ^{109}Ag NMR spectra of the samples $x=0.33$ (a), and $x=0.25$ (b) heated at 140 °C for 15 h.

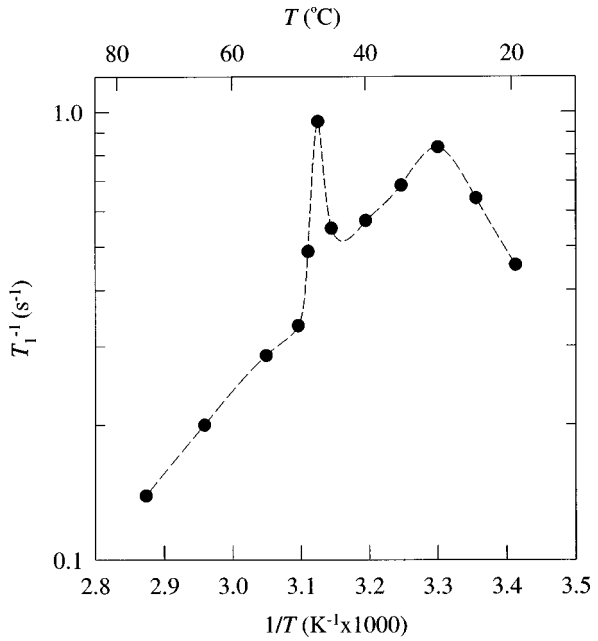

FIG. 8. ^{109}Ag NMR spin-lattice relaxation rate $1/T_1$ of the sample $x=0.25$. The dashed line is only a guide for the eyes.

reported in Ref. 12. Similar NMR patterns are found in all samples where the 2:1 glassy phase underwent crystallization. The sample $x=0.25$ displays the peak of crystalline AgI in addition to the CSA powder pattern of the 2:1 phase.

The singularities of the pattern of Fig. 7(a), allow us to estimate the principal components of the screening tensor.[24] We obtain $\sigma_{11}\cong -620$ ppm, $\sigma_{22}\cong -501$ ppm and $\sigma_{33}\cong -484$ ppm. Due to the low signal-to-noise ratio an error of 5% is estimated. From Eqs. (4)–(6) we obtain the values $\sigma^*=-535$ ppm, $\delta_{CS}=51$ ppm, and $\eta_{CS}=2.33$. Here, the chemical shift tensor of ^{109}Ag is assigned in a silver oxysalt compound. Tansho *et al.* found $\delta_{CS}\sim 350$ ppm in a low-temperature crystalline phase of the silver ionic conductor Ag_9GaSe_6.[25] Villa *et al.*[8] estimated the intensity of the anisotropic interaction in $Ag_2O\cdot B_2O_3$ glass to be ~180 ppm at 325 K.

V. DYNAMIC INFORMATION

While there is no doubt that linewidth and spin-lattice relaxation are determined by the ion diffusion, it is not clear if the same nuclear interaction is responsible for the temperature behaviour of both linewidth and T_1. Although it was argued that time-dependent anisotropic chemical shift is the dominant mechanism for spin-lattice relaxation in silver-based glasses,[9,26] other mechanisms cannot, in principle, be ruled out such as (i) Ag-I dipolar or pseudodipolar coupling, (ii) modulation by ionic motion of ^{107}Ag-^{109}Ag or ^{109}Ag-I scalar interaction (relaxation of the first kind), or also (iii) Ag-I scalar interaction coupled with iodine quadrupolar relaxation (relaxation of the second kind). Chung *et al.*[10] showed by order-of-magnitude calculations that mechanisms (i) and (iii) can be ruled out in silver borate glasses. In contrast, scalar coupling relaxation of the first kind may be significant. The same considerations they made for borates are applicable to molybdates.

Figure 8 shows the spin-lattice relaxation rate, $1/T_1$, of the sample $x=0.25$ vs the reciprocal temperature. A first maximum is found at 303 K, which indicates the transition to the extreme narrowing regime. Near the maximum it is acceptable to let the spectral density $J(\omega_0)$ have the Debye form $\tau_c/(1+\omega_0^2\tau_c^2)$,[27] and we obtain for the correlation time of the ionic motion $\tau_c=1/\omega_0$. We can apply Eq. (10) to the scalar coupling of the first kind between Ag and I. If we assume for the Ag-I scalar coupling constant the reasonable value $J\sim 1$ kHz,[28] we obtain $T_{1,\min}=1.75$ s, in good agreement with our experimental value of 1.2 s. By using a Hahn-echo sequence we obtained $T_2=110\pm 11$ ms. Since $T_1/T_2 \gg 7/6$ we can conclude that scalar coupling of the first kind, rather than CSA, seems to determine the relaxation in silver molybdate glasses, at least near room temperature.

The relaxation rate curve of Fig. 8 displays a second maximum at 320 K, the temperature at which $x=0.25$ undergoes the glass transition.[12] This maximum, as a consequence, is put into relation with the onset of a further motional process which involves nearly all the silver cations. At a first approximation, spin-lattice relaxation rates due to different mechanisms are additive

$$T_1^{-1}=\sum_j T_{1j}^{-1}. \tag{11}$$

Below the T_g, the observed spin-lattice relaxation rate $1/T_{1,gl}$ is given by

$$\frac{1}{T_1 gl}=\frac{p}{T_{1\ \mathrm{mob}}}+\frac{1-p}{T_{1\ \mathrm{imm}}}, \tag{12}$$

where p is the fraction of mobile Ag^+, while $T_{1,\mathrm{mob}}$ and $T_{1,\mathrm{imm}}$ are the relaxation times of mobile and immobile (or less mobile) cations, respectively. It is assumed that each spin will sample both behaviors during a T_1 period. Above the glass transition, all the Ag^+ are mobile and we have

$$\frac{1}{T_{1\ \mathrm{liq}}} = \frac{1}{T^{*}_{1\ \mathrm{mob}}}. \tag{13}$$

If we neglect $1/T_{1,\mathrm{imm}}$ with respect to $1/T_{1,\mathrm{mob}}$ and consider $T^{*}_{1,\mathrm{mob}} \cong T_{1,\mathrm{mob}}$, which is reasonable in the considered temperature range, we obtain $p \cong 0.875$. In our previous ^{109}Ag NMR work,[29] we estimated the fraction of mobile cations to be less than 50%. However, those data were obtained on samples prepared just one day before the measurements. An experiment performed two months later (i.e., at the same time of the T_1 measurements here reported) gave a mobile fraction $p > 80\%$, in agreement with the above results. On the basis of this evidence, and following the suggestions of Ref. 8, we can model the dynamics of our spin system in terms of a distribution of barrier heights for the Ag^+ jumps, rather than in terms of two true chemically defined silver species. Under these assumptions, we argue that the sample stored at $\sim$20 °C below its T_g has undergone structural rearrangements that determined some changes in the barrier heights distribution.

In systems characterized by a rate-activated process, the correlation time τ_c, which determines the NMR spectral density can be expressed in an Arrhenian form[9]

$$\tau_c = \tau_\infty e^{E_a/kT}, \tag{14}$$

where E_a is the activation energy, and τ_∞ is the prefactor. By fitting the data reported in Fig. 8 we obtain $E_a = 0.31$ eV in the region 300–315 K, and $E_a = 0.29$ eV above the glass transition. Values in the range 0.19–0.23 eV were obtained form conductivity measurements near room temperature,[3,5,17,30] whereas $E_a = 0.27$ eV was obtained at low temperature.[4] The value we obtained from NMR relaxation is larger by $\sim$30% than the conductivity-related data. This can be explained by supposing that T_1 mechanism essentially probes the long-range ions translation, whereas the conductivity experiments measure a sort of average of local and long-range motions.[9] On the other hand, our conclusions are in agreement with the fact that spin-lattice relaxation is dominated by scalar coupling of the first kind (a long-range interaction described by particle-particle correlation), rather than by CSA (a short-range interaction described by particle-site correlation).

VI. CONCLUSIONS

We have investigated by ^{109}Ag solid-state NMR both the structure and the ion dynamics of the system AgI Ag_2MoO_4. The following conclusions can be drawn:

(1) Increasing the AgI fraction causes the formation of oxyiodide sites with an increasing I/O ratio. The existence of AgI clusters can be ruled out, in agreement with the findings of Minami and Tanaka,[3] and Kamitsos *et al.*[7] Outside the glass-formation region, $0.2 < x < 0.4$, a glassy phase of composition near 0.66 AgI-0.33 Ag_2MoO_4 (2:1) is always formed, which is accompanied by crystalline β-AgI or Ag_2MoO_4.

(2) Inside the glass formation region we observe a single NMR peak. We are not able, at present, to operate a conclusive choice between a homogeneous phase or the motional average of different chemical environments. In principle, NMR at the magic angle technique at low temperature could address this question, but the experiments are very difficult to carry out. A subtle indication favoring the existence of the 2:1 glass over the entire composition range is given by the sample $x = 0.40$, at the boundaries of the glass-formation region, that displays the peaks of two glassy phases of composition $x \sim 0.3$ and $x \sim 0.4$.

(3) The chemical shift anisotropy tensor of the 2:1 crystallized phase has been assigned. The anisotropy is $\sim$70 ppm, which is an order-of-magnitude lower than the isotropic chemical shift range observed in these glasses.

(4) The spin-lattice relaxation inside the glass-formation region seems to be controlled by Ag-I scalar coupling of the first kind, rather than by chemical shift anisotropy. This may account for the larger activation energies which are given by NMR T_1 with respect to those obtained by dc conductivity experiments.

(5) The existence of two maxima in the spin-lattice relaxation rate curve points towards Ag^+ populations with different mobility, probably related to the existence of local environments where different I/O ratios are dynamically experienced by the ions. However, we had preliminary evidence of a structural relaxation taking place at room temperature in a matter of months. Experiments are in progress to correlate these NMR results with variations of dc conductivity and, possibly, formation of quasicrystalline AgI domains.

ACKNOWLEDGMENTS

Some helpful discussions with Professor Marco Villa are gratefully acknowledged. The measurements were performed at ''Centro Grandi Strumenti'' of University of Pavia.

*Author to whom correspondence should be sent. Electronic address: mustarelli@matsci.unipv.it

[1] G. Chiodelli, A. Magistris, and A. Schiraldi, Electrochim. Acta **19**, 655 (1974).
[2] T. Minami, H. Nambu, and M. Tanaka, J. Am. Ceram. Soc. **60**, 283 (1977).
[3] T. Minami and M. Tanaka, J. Non-Cryst. Solids **38&39**, 289 (1980).
[4] D. P. Almond, G. K. Duncan, and A. R. West, J. Non-Cryst. Solids **74**, 285 (1985).
[5] St. Adams, K. Hariharan, and J. Maier, Solid State Ionics **75**, 193 (1995).
[6] J. Swenson, R. L. McGreevy, L. Börjesson, J. D. Wicks, and W. S. Howells, J. Phys.: Condens. Matter **8**, 3545 (1996).
[7] E. I. Kamitsos, J. A. Kapoutsis, G. D. Chryssikos, J. M. Hutchinson, A. J. Pappin, M. D. Ingram, and J. A. Duffy, Phys. Chem. Glasses **36**, 141 (1995).
[8] M. Villa, G. Chiodelli, A. Magistris, and G. Licheri, J. Chem. Phys. **85**, 2392 (1986).
[9] W. Martin, H. J. Bishof, M. Mali, J. Roos, and D. Brinkmann, Solid State Ionics **18&19**, 421 (186).
[10] S. H. Chung, K. R. Jeffrey, J. R. Stevens, and L. Börjesson, Phys. Rev. B **41**, 6154 (1990).

[11] S. H. Chung, K. R. Jeffrey, J. R. Stevens, and L. Börjesson, Solid State Ionics **40/41**, 279 (1990).
[12] C. Tomasi, P. Mustarelli, and A. Magistris, Solid State Chem. (to be published).
[13] R. Kohlmuller and J.-P. Faurie, Bull. Soc. Chim. Fr. **11**, 4379 (1968).
[14] See, for example, M. Mehring, *High Resolution NMR Spectroscopy in Solids* (Springer-Verlag, Berlin, 1976).
[15] N. Bloembergen and T. J. Rowland, Phys. Rev. **55**, 1679 (1955).
[16] A. Abragam, *The Principles of Nuclear Magnetism* (Oxford University Press, London, 1961).
[17] J. Sanz, P. Herrero, R. Rojas, J. M. Rojo, S. Rossignol, J. M. Réau, and B. Tanguy, Solid State Ionics **82**, 129 (1995).
[18] T. Minami, K. Matsuda, and M. Tanaka, Solid State Ionics **3/4**, 93 (1981).
[19] T. Minami, K. Matsuda, and M. Tanaka, J. Electrochem. Soc. **128**, 100 (1981).
[20] J. Kawamura and M. Shimoji, J. Non-Cryst. Solids **88**, 295 (1986).
[21] F. Rocca, A. Kuzmin, P. Mustarelli, C. Tomasi, and A. Magistris (unpublished).
[22] H. Looser and D. Brinkmann, J. Magn. Reson. **64**, 76 (1985).
[23] C. W. Burges, R. Koschmieder, W. Sahm, and A. Schwenk, Z. Naturforsch. A **28a**, 1753 (1973).
[24] See, for example, G. Engelhardt and D. Michel, *High-Resolution Solid-State NMR of Silicates and Zeolites* (Wiley, Chichester, 1987), p. 39.
[25] M. Tansho, H. Wada, M. Ishii, and Y. Onoda, Solid State Ionics **86–88**, 155 (1996).
[26] J. Roos, D. Brinkmann, M. Mali, A. Pradel, and M. Ribes, Solid State Ionics **28–30**, 710 (1988).
[27] N. Bloembergen, E. M. Purcell, and R. V. Pound, Phys. Rev. **73**, 679 (1948).
[28] B. Lindman and S. Forsén, in *NMR and the Periodic Table*, edited by R. K. Harris and B. E. Mann (Academic, London, 1978), p. 421.
[29] P. Mustarelli, C. Tomasi, A. Magistris, and M. Cutroni, J. Non-Cryst. Solids (to be published).
[30] J. Kawamura and Y. Oyama, Solid State Ionics **35**, 311 (1989).